ON NONSPECULAR REFLECTION OF BOUNDED BEAMS FOR LAYERED HALF SPACES UNDER WATER

D.B. Bogy and S.M. Gracewski

Department of Mechanical Engineering
University of California
Berkeley, CA 94720

ABSTRACT

We study the recently derived reflection coefficient for plane waves in a liquid that are incident on the liquid-solid interface of a solid half space which consists of a single layer of one elastic material bonded to a substrate of a different material. Plots of the magnitude of the reflection coefficient versus the incident angle are presented for several sets of material parameters and values of frequency f and layer thickness d. The use of the results presented for the study of nonspecular reflection of bounded acoustic beams is of primary interest. We therefore seek to identify all the critical incidence angles for nonspecular reflection.

We also investigate, in particular, the surface wave propagation for the case of a stiff layer on a soft half space, and we find that the purely propagating mode cuts off with increasing fd (f is the frequency and d the layer thickness) when its speed reaches approximately the shear wave speed of the substrate, as reported in the literature. However, as fd increases further, a leaky mode appears that approaches the Rayleigh wave for the layer. This leaky mode is also associated with nonspecular reflection for large enough fd.

INTRODUCTION

Nonspecular reflection of bounded underwater ultrasonic beams from a plane interface between the water and an elastic solid has been studied in several papers over the last 30 years. Schoch[1] demonstrated the phenomenon for water on a homogeneous elastic solid, which we will refer to as the LS structure, after predicting it on the basis of a similar occurrence in optics known as the Goos-Hänchen[2]

effect. Schoch[3] also studied the case of a solid layer submersed in water, which we will call the LSL structure, and he presented the first, but somewhat incomplete, theoretical explanation of the lateral displacement of the reflected beam. Schoch's analysis was improved in Brekhovskikh,[4] where layered structures were also considered. The theoretical explanation of all the aspects of nonspecular reflection of bounded beams in the LS case was presented in Bertoni and Tamir.[5] A similarly thorough treatment of the LSL case was contained in Pitts,[6] and the related papers Pitts et al.[7] and Plona et al.[8]

The problem of nonspecular reflection from a layered half space, consisting of a thin layer of one material bonded to a thick substrate of a different material, has been studied recently by Chimenti et al.,[9] and Chimenti and Nayfeh.[10] We will refer to this as the LSS structure. In Ref. 9 the loading case of copper on stainless steel was studied. Nonspecular reflections were measured and calculated corresponding to the lowest Rayleigh mode. Reference 10 considered also the stiffening case of chromium on stainless steel. They found experimentally that the wave did not cut off with increasing fd (where f is the frequency and d is the layer thickness) at the layer shear wave speed as expected. Instead it "persists as a leaky wave up to about 130% of this cutoff" value of fd.[10]

The LSS structure was also considered in Bogy and Gracewski.[11] The reflection coefficient for plane waves was derived for several models of the layered structure. These included some approximate plate theories for the layer as well as the case in which the layer is modeled by exact linear elasticity theory. These reflection coefficients were given in algebraic form, as opposed to a form containing determinants, and several limiting cases were studied.

In this paper the reflection coefficient of the exact theory derived in Ref. 11 is studied numerically for several material combinations and values of fd. The parameters of the layer are held fixed at those for stainless steel while the half space substrate parameters range from stainless steel to brass and further to water. This study presents a unifying picture between the LS, LSL, and LSS cases. We also explain the propagating wave behavior for the stiffening case over the entire range of fd. In particular, we show how the Rayleigh mode for the layer is approached as fd increases. This paper is an abbreviated version of Bogy and Gracewski.[12]

THE REFLECTION COEFFICIENT

The reflection coefficient derived in Ref. 11 for the LSS structure in Fig. 1 has the form

$$r = e^{-i2P_L}(N/D), \tag{1}$$

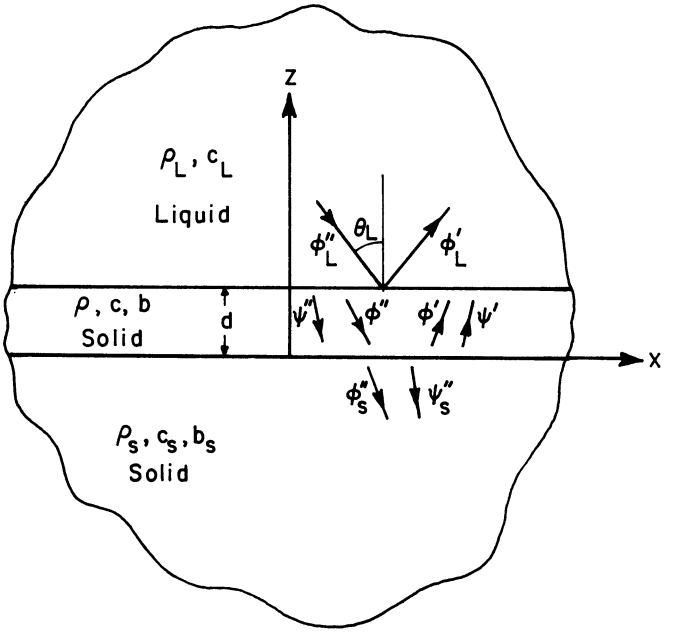

Fig. 1. Liquid-solid layer-solid structure with incident plane wave from liquid.

where

$$
\begin{aligned}
\left(\frac{N}{D}\right) = {} & \{2r^2 S_{2\theta} S_{2\gamma} C_{2\gamma}^2 (1 - C_P C_Q) + (C_{2\gamma}^4 + r^4 S_{2\theta}^2 S_{2\gamma}^2) S_P S_Q \\
& - (\pm) i (Z_{\theta_L}/Z_\theta)(C_{2\gamma}^2 C_P S_Q + r^2 S_{2\theta} S_{2\gamma} S_P C_Q)\} Z_\theta Z_\gamma (1 + T_{\theta_S} T_{\gamma_S}) \\
& + \{i(C_{2\gamma}^2 C_P S_Q + r^2 S_{2\theta} S_{2\gamma} S_P C_Q) - (\pm)(Z_{\theta_L}/Z_\theta) S_P S_Q\} Z_\gamma Z_{\theta_S} \\
& + \{-[S_{4\gamma}(C_{2\gamma} - r^2 T_\theta S_{2\theta})(1 - C_P C_Q) + 2(r^2 S_{2\theta} S_{2\gamma}^2 - T_\theta C_{2\gamma}^3) S_P S_Q] \\
& + (\pm) i 2 \left(\frac{Z_{\theta_L}}{Z_\theta}\right)\left(\frac{Z_\theta}{Z_\gamma}\right)(r^2 S_{2\gamma} S_P C_Q - T_\gamma C_{2\gamma} C_P S_Q)\} Z_\gamma Z_{\gamma_S} (S_{2\gamma_S} - T_{\theta_S} C_{2\gamma_S}) \\
& + \{i(C_{2\gamma}^2 S_P C_Q + r^2 S_{2\theta} S_{2\gamma} C_P S_Q) + (\pm)(Z_{\theta_L}/Z_\theta) C_P C_Q\} Z_\theta Z_{\gamma_S} \\
& + \{-[4 S_\gamma^2 C_{2\gamma} + (C_{2\gamma}^2 + 4 S_\gamma^4) C_P C_Q - (T_\gamma T_\theta C_{2\gamma}^2 + r^2 S_{2\theta} S_{2\gamma}) S_P S_Q] \\
& - (\pm) i (Z_{\theta_L}/Z_\theta)(S_P C_Q + T_\theta T_\gamma C_P S_Q)\} Z_{\gamma_S} Z_{\theta_S} \Delta_S \ . \qquad (2)
\end{aligned}
$$

in which the upper choice of sign is used in the expression for the numerator N and the lower choice with the denominator D. The following notation is also employed:

$$P = \alpha d, \quad Q = \beta d, \quad P_L = \alpha_L d, \quad r = b/c, \quad Z_\theta = \rho c/C_\theta,$$
$$Z_\gamma = \rho b/C_\gamma \quad , \tag{3}$$

where ρ_L, c_L represent the density and longitudinal wave speed in the fluid while ρ, c, b and ρ_S, c_S, b_S represent the density, longitudinal and shear wave speeds in the layer and substrate, respectively, θ_L, θ, θ_S and γ, γ_S are the angles between the normal to the interfaces and the longitudinal wave vectors k_L, k, k_S and shear wave vectors κ, κ_S, respectively. The normal components of these wave vectors are denoted by α_L, α, α_S and β, β_S, respectively. The tangential components of all the wave vectors are the same, and are denoted by σ. Δ_S is the Rayleigh function for the half space

$$\Delta_S = C_{2\gamma_S}^2 + r_S^2 S_{2\theta_S} S_{2\gamma_S} \quad , \tag{4}$$

and we have employed the shorthand notation

$$S_\theta = \sin\theta, \quad C_\theta = \cos\theta, \quad T_\theta \tan\theta, \quad Ct_\theta = \cot\theta. \tag{5}$$

DEPENDENCE OF THE REFLECTION COEFFICIENT ON MATERIAL PARAMETERS

The reflection coefficient for infinite plane waves given in the previous section can be used in the mathematical representation of reflected bounded beams in the manner described in Ref. 5. Such beams will be reflected in a nonspecular manner if the incident beam excites a leaky interface wave. These are propagating modes in the absence of the liquid half space and they are defined by real values σ^* that are roots of the frequency equation studied in Farnell and Adler.[13] Both N and D in Eq. (2) reduce to this frequency equation in the limit where the fluid half space becomes a vacuum. In the presence of the liquid these roots σ^* of $D(\sigma)$ in Eq. (2) move somewhat away from the real axis and the modes have a corresponding decay in amplitude and are called leaky modes. We have found that roots determining propagating modes for one particular material combination may also move away from the real axis as the material parameters change. Farnell and Adler[13] considered only propagating modes for the layer-half space, i.e., they find only the real roots σ^*. We will show that for certain layer-half space material combinations it is possible for roots to occur arbitrarily close to the real axis in the complex σ-plane in the absence of the upper liquid half space, and while the modes are not propagating in the sense of Ref. 13, their amplitude decay is small and they do define angles of incidence for nonspecular reflection of bounded beams.

One way to determine the poles and zeros of the reflection coefficient in the complex σ-plane is to search numerically using the principal of the argument[6] or a Newton-Raphson technique.[9] We have found that when a pole of R in the complex σ-plane is sufficiently near the real axis to correspond to a mode that causes nonspecular reflections, it will be associated with a zero also near the real axis. The poles always have positive imaginary parts in the presence of the liquid, but the zeros can have positive or negative imaginary parts. A zero usually has an imaginary part that is less than the imaginary part for the corresponding pole. The zero-pole pairs coalesce in the limit as the liquid vanishes. If they coalesce to a real value in this limit they represent modes that propagate without decay in amplitude. If they coalesce to complex values they represent leaky modes that decay as they propagate.

Since the zeros of the reflection coefficient occur below the poles and the poles always have positive imaginary parts, we find that the real parts of the zero-pole pairs near the real σ-axis can be observed by merely calculating $|R|$ along a path just below this axis. The reflection coefficient is a function of the material parameters, of fd (or ωd), and of θ_L, the incident angle in the liquid. Figs. 2a-b present a study of $|R|$ versus $\sin\theta_L$ for fixed fd (fd = 5 MHz.mm), and varying material parameters. In all cases the function $|R|$ is evaluated along the path $\sigma = \sigma_R - i0.001$, $0 \leq \sigma_R \leq k_L$, and $\sin\theta_L = \sigma_R/k_L$. The material parameters in Figs. 2a-2b are varied between those for water (W), brass (B), and stainless steel (S). We designate the water-stainless steel layer-brass half space as WSB. Each of the Figs. 2a-2b shows $|R|$ versus $\sin\theta_L$ for six different sets of material parameters that represent equal increments in parameter space between the top and bottom graphs. (When the substrate is represented as water, the shear wave number is arbitrarily set at $(1000)^{\frac{1}{2}}$, which is found numerically to give virtually the same results as water if ρ_S and k_S also correspond to water.) All of the six curves in each figure are plotted to the same scale. The vertical origins are displaced so the curves will not superimpose. The amount of displacement can be seen from the values near $\sin\theta_L = 1$ where the value of $|R|$ for all curves is one.

In Fig. 2a the material parameters vary between WSS and WSB and in Fig. 2b they vary between WSB and WSW. The parameter end values of WSS and WSW correspond to previously studied cases, and both are discussed extensively in Ref. 6 (the layer is brass there), where they are designated the Liquid-Solid (LS) case and the Liquid-Solid-Liquid (LSL) case, respectively. The plot of $|R|$ versus $\sin\theta_L$ for the LS case (top curve) can also be found in Ref. 4 and elsewhere. In Fig. 2a the top curve, for WSS, is in agreement with these previously published results and this case is characterized by four features: the value for $\theta_L = 0$; the cusp where $|R|$ first rises to one, which corresponds to the longitudinal wave number for the solid;

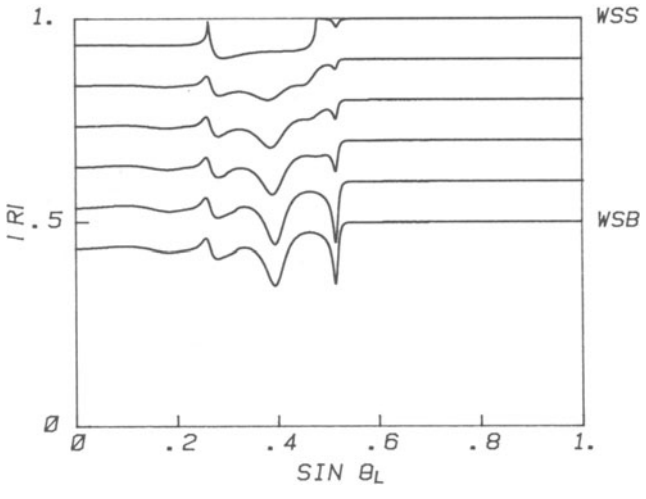

Fig. 2a. Modulus of reflection coefficient, $|R|$, versus incident angle $\sin\theta_L$ for various material combinations between water (W), brass (B), and stainless steel (S), for frequency-thickness, fd, fixed at 5 MHz.mm (f=4 MHz, d=1.25mm). The parameters used were:

	ρ(gm/cm^3)	c(km/sec)	b(km/sec)
W (water)	1	1.49	-
B (brass)	8.5	4.70	2.11
S (s.steel)	7.9	5.69	3.13

the kink where the value of $|R|$ next rises to one, which corresponds to the shear wave number of the solid; and the slight dip just past the kink, which corresponds to the Rayleigh wave number for the solid. In the complex σ-plane there is only one zero-pole pair near the real axis for this case and they are complex conjugates. They move to the real axis at the Rayleigh wave number in the limit where the upper liquid becomes a vacuum. It can be shown that $|R| = 1$ beyond the shear wave angle kink. The slight dip that occurs at the Rayleigh wave angle is due to our evaluation of $|R|$ along the path σ_R -i0.001 rather than along the real σ-axis, and the fact that the zero occurs in the lower quadrant.

The plot of $|R|$ versus $\sin\theta_L$ for the LSL case (bottom curve in Fig. 2b) can be found in Refs. 6 and 7, for a brass layer. It is

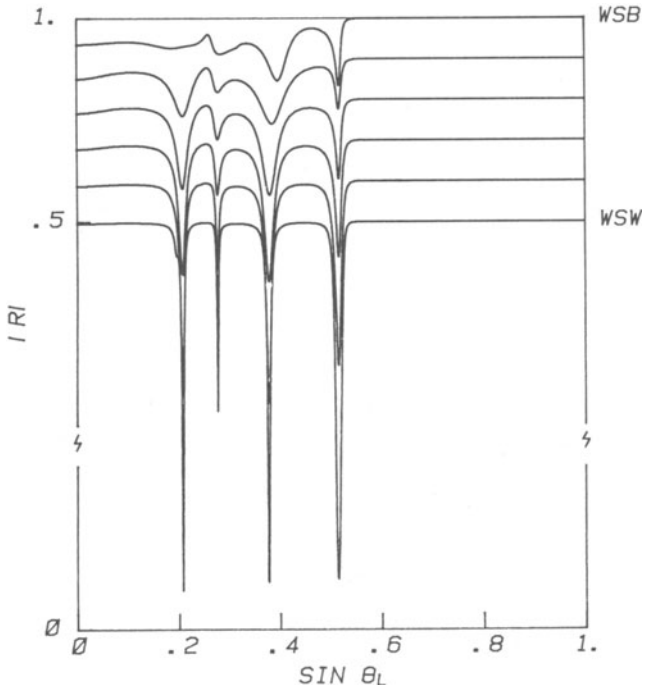

Fig. 2b. (same caption as Fig. 2a.)

characterized by the sharp spikes that drop to zero together with the dip that occurs at about the Rayleigh angle. As discussed in Refs. 6 and 7 the spikes correspond to the Lamb modes for the plate at the particular value of fd (fd = 5 MHz.mm here). They are associated with zero-pole pairs of R which are not complex conjugates in the σ-plane but for which the zeros are real and the poles lie above the zeros with the same real parts. In the limit as the liquid on both sides of the plate becomes a vacuum, the poles move to the real axis at the corresponding zeros. The last dip in $|R|$, which occurs near the Rayleigh angle, corresponds to the lowest plate mode whose velocity approaches the Rayleigh velocity at high values of fd.

The set of graphs in Fig. 2b indicates that as the lower half space parameters change from water to brass the zero-pole pairs corresponding to the Lamb modes move away from the axis. Indeed, we find that they move up together into the upper quadrant far enough from the real axis so they are no longer associated with a propagating or leaky mode. The zero and pole trajectories relevant to the approximation of R depend on the material parameters in a rather complicated manner, which requires changes in the choice of branches of multi-valued terms in R. A complete analysis of the zero and pole trajectories will be presented in a later paper.

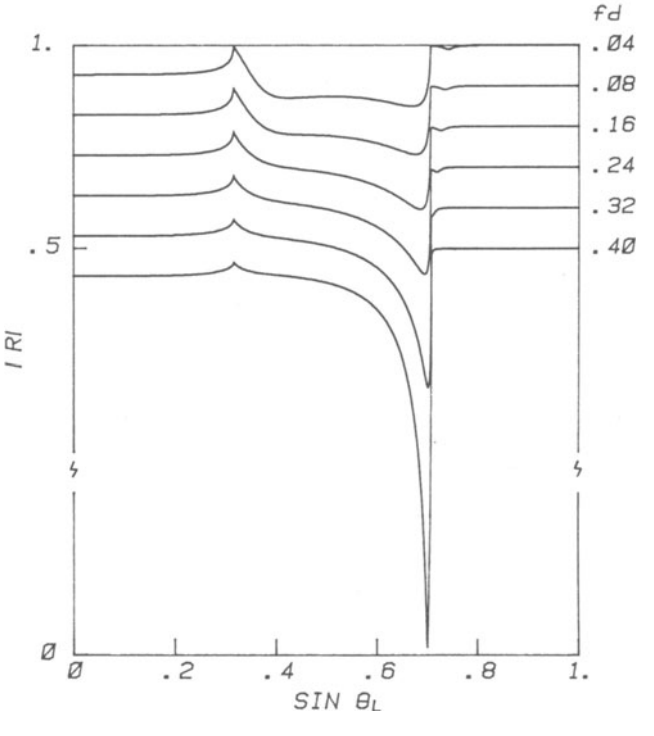

Fig. 3a. Modulus of reflection coefficient, $|R|$, versus incident angle $\sin\theta_L$ for WSB (see caption for Fig. 2a) for various values of fd.

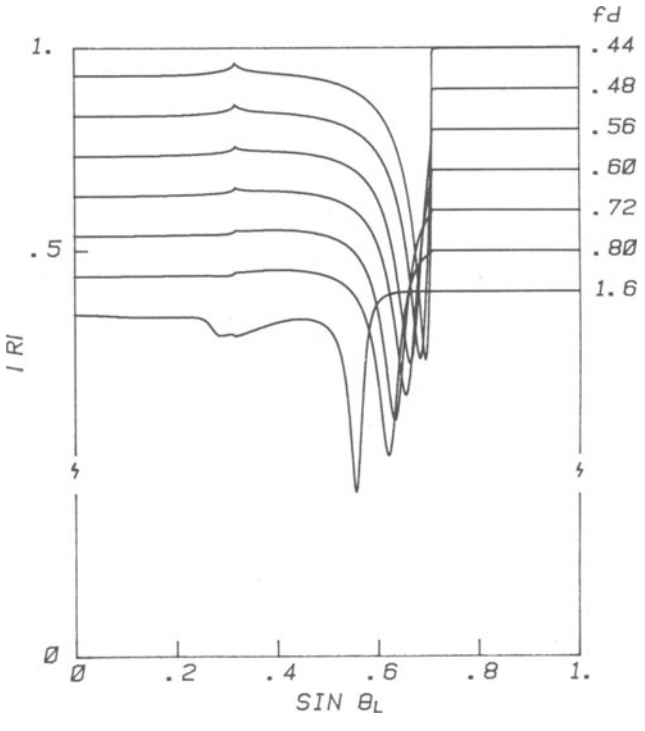

Fig. 3b. (same caption as Fig. 3a.)

DEPENDENCE OF THE REFLECTION COEFFICIENT ON FREQUENCY-THICKNESS

In this section we study the reflection coefficient as fd changes for the stiffening case of WSB. In Figs. 3a-d fd varies from 0.04 to 12 MHz.mm. According to Ref. (13) only a single Rayleigh type mode exists and its velocity varies between the Rayleigh velocity and the shear velocity of the substrate (brass) as fd increases. As the shear velocity is reached the mode propagates without decay of amplitude with depth and thus loses its surface wave character. As fd increases beyond this value no purely propagating mode is possible. The top curve in Fig. 3a for fd = 0.04 is indistinguishable from the LS case for water and brass. The

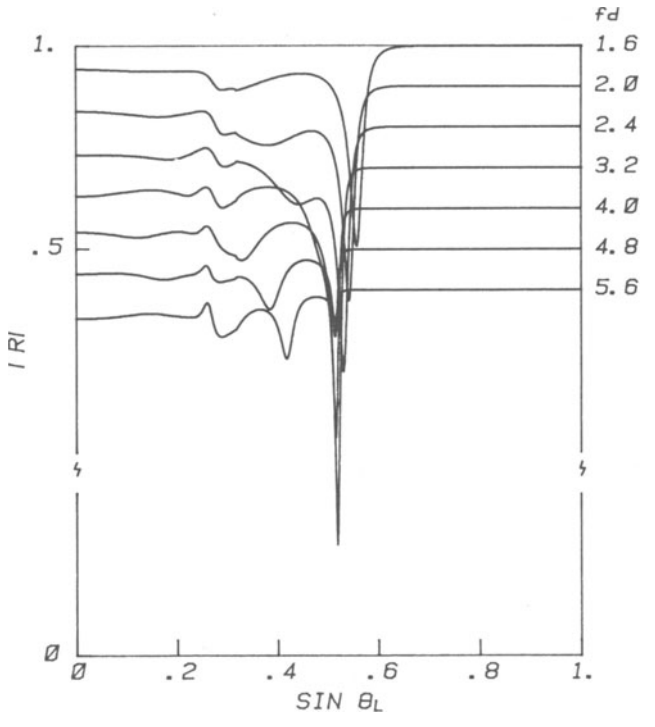

Fig. 3c. (Same caption as Fig. 3a.)

slight dip at the Rayleigh wave number is again visible due to the offset of the path of evaluation of $|R|$. As fd increases from 0.04 this Rayleigh zero-pole pair is seen in Fig. 3a to move to the left and it reaches the real axis at about fd = 0.40. We found that the zero-pole pair remained complex conjugates but approached the real axis near, but not exactly at, the brass shear wave number (see Fig. 4). Up to fd $\simeq$ 0.38 they would approach the real axis if the upper liquid were to become a vacuum. The pair corresponding to 0.38 moves to the brass shear wave number. As fd increases beyond 0.40 the zero moves into the upper quadrant of the σ-plane and becomes paired with a different pole, forming a leaky Lamb-type mode. This zero-pole pair would not approach the real axis if the upper liquid were to become a vacuum. Therefore it is not included in

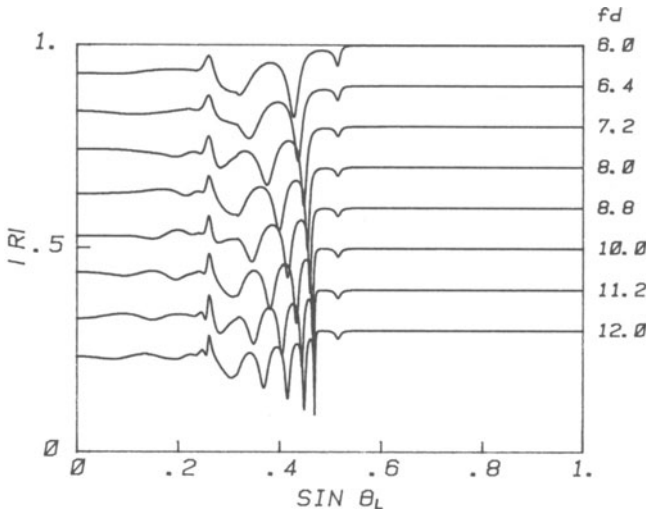

Fig. 3d. (Same caption as Fig. 3a.)

the propagating modes in Ref. 13. As fd increases still more the zero moves down and crosses the real axis (at about fd = 3.3) as indicated in Fig. 3c and Fig. 4. As fd continues to increase this zero-pole pair approaches the Rayleigh mode for stainless steel, i.e., the zero-pole pair approaches complex conjugates at the Rayleigh wave number for stainless steel. Evidently this limit is never exactly reached as fd increases, but it is essentially attained by fd = 6.0, as can be seen in Fig. 3d and Fig. 4. Also, if the upper liquid were to approach a vacuum, this zero-pole pair would not exactly reach the real axis in the range between the shear wave number for the brass substrate and the Rayleigh wave number for the stainless steel layer. Thus this mode is not identified as a propagating mode in Ref. 13. Nevertheless, we found that nonspecular reflection of bounded beams is predicted at the incidence angle corresponding to this mode. However, for fd < 3.0 the nonspecular part of the reflected beam may be too faint to be experimentally observed. Also, in practical terms the Rayleigh waves observed in the laboratory are actually related to this mode for large fd since the laboratory "half space" always has a finite thickness d.

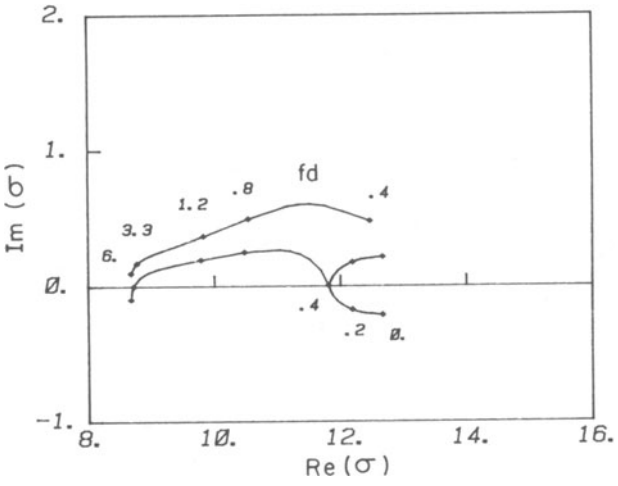

Fig. 4. Trajectory of zero-pole pair associated with propagating Rayleigh mode ($0 \leq fd \leq 0.4$ with $Im(\beta_s) > 0$) and leaky Lamb-type mode becoming Rayleigh-type mode ($fd > 0.4$ with $Re(\beta_s) > 0$).

Fig. 3d indicates that several leaky Lamb-type mode zero-pole pairs appear just to the left of the stainless steel layer shear wave number as fd increases. The curve for fd = 12 shows five such modes. These modes are too leaky to be excited by bounded beams.

Therefore, for the stiffening case of WSB we find the Rayleigh type mode exists with speeds varying, as fd increases from zero, between the Rayleigh wave speed and the shear wave speed of brass. It cuts off at this speed as a purely propagating mode and becomes a leaky mode. As fd increases more the mode becomes more leaky and then comes back as a less leaky mode, and it approaches a propagating mode with the Rayleigh wave speed of stainless steel. This behavior is substantiated by Fig. 4, which shows the discussed zero-pole trajectories.

DISCUSSION AND CONCLUSIONS

In this study we have presented a unifying picture between the LS, LSL, and LSS reflection coefficients by varying the material

parameters for the LSS case, which includes the other two as special cases. The technique of evaluating $|R|$ just below the real axis in the complex σ-plane was used to locate the incident angles where nonspecular reflection of bounded beams should be anticipated. This requires considerably less computational effort than searching for all the zeros and poles of R. On the other hand, a thorough understanding of the analytic structure of R and the dependence of this structure on the various parameters requires the computation of the zero and pole trajectories corresponding to the changes in these parameters.

The study of the stiffening case of WSB (water-stainless steel-brass) revealed that the Rayleigh mode cuts off as fd increases from zero near, but not at, the shear wave speed for brass (at fd $\simeq$ 0.4) MHz.mm). As fd increases further a leaky mode appears, first with a Lamb mode character and then approaching the Rayleigh mode for the stainless steel layer (at fd $\simeq$ 6 MHz.mm). This is illustrated in Figs. 3a-d and Fig. 4.

It should be noted that the zero-pole pair to the left of the cut-off point in Fig. 4 belongs to a different branch of R than does the pair to the right. The left portion has $\mathrm{Re}(\alpha_L, \alpha, \beta, \beta_S) > 0$, $\mathrm{Im}(\alpha_S) > 0$, while the right portion has $\mathrm{Re}(\alpha_L, \alpha, \beta) > 0$, $\mathrm{Im}(\alpha_S, \beta_S) > 0$. It should also be pointed out that the zero-pole pair comes together, from the right as fd increases, slightly to the left of κ_S, the shear wave number of the substrate, which is also a branch point. We found that for a denser liquid this merging point of the zero and pole moves even further to the left. As the liquid becomes less dense than water, and approaches a vacuum, this point moves to the right and approaches κ_S.

ACKNOWLEDGEMENT

This research was partially supported by the National Science Foundation under Grant CME-8017840 and by Lawrence Livermore National Laboratory Purchase Order No. 7734501 to the University of California, Berkeley. One of us, S.M.G., would like to acknowledge support by an IBM Predoctoral Fellowship.

REFERENCES

1. A. Schoch, "Seitliche Versetzung eines total reflektierten Strahls bei Ultraschallwellen," Acustica, 2, 18-19, 1952.
2. F. Goos and H. Hänchen, "Ein neuer und fundamentaler Versuch zur Totalreflexion," Ann. Phys. (Leipzig), 1, 337, 1947.
3. A. Schoch, "Der Schalldurchgang durch Platten," Acustica, 2, 1-17, 1952.
4. L.M. Brekhovskikh, Waves in Layered Media, Academic Press, New York, 1960.

5. H.L. Bertoni and T. Tamir, "Unified theory of Rayleigh-Angle phenomena for acoustic beams at liquid-solid interfaces," Appl. Phys., 2, 157-172, 1973.
6. L.E. Pitts, "A unified theoretical description of ultrasonic beam reflections from a solid plate in a fluid," Ph.D. Thesis, Georgetown University, 1976.
7. L.E. Pitts, T.J. Plona and W.G. Mayer, "Theory on nonspecular reflection effects for an ultrasonic beam incident on a solid plate in a liquid," IEEE Trans. Sonics and Ultrasonics, SU-24, 101-108, 1977.
8. T.J. Plona, L.E. Pitts and W.G. Mayer, "Ultrasonic bounded beam reflection and transmission effects at a liquid/solid plate/liquid interface," J. Acoust. Soc. Am., 59, 1324-1328, 1976.
9. D.E. Chimenti, A.H. Nayfeh and D.L. Butler, "Leaky Rayleigh waves on a layered halfspace," J. Appl. Phys., 53, 170-176, 1982.
10. D.E. Chimenti and A.H. Nayfeh, "Leaky Rayleigh waves at a layered half space--fluid interface," Proc. of Ultrasonic Symp., IEEE, 291-294, 1981.
11. D.B. Bogy and S.M. Gracewski, "Reflection coefficient for plane waves in a fluid incident on a layered half-space," J. Appl. Mech., to appear.
12. D.B. Bogy and S.M. Gracewski, "On the plane wave reflection coefficient and nonspecular reflection of bounded beams for layered half spaces under water," J. Acoust. Soc. Am., submitted.
13. G.W. Farnell and E.L. Adler, "Elastic wave propagation in thin layers," in Physical Acoustics, Vol. 9, 35-127, Academic Press, New York, 1972.